Limnology
https://doi.org/10.1007/s10201-024-00762-9

RESEARCH PAPER

The sources of nitrate exported from a watershed containing mixed forest, paddy fields, and urban areas in Japan: differences between baseflow conditions and rainfall events

Ken'ichi Osaka[1,2] · Megumi Takatsu[3] · Takaaki Ishibashi[4,5] · Shinsho Chishiro[4] · Takashi Nakamura[6]

Received: 20 September 2023 / Accepted: 10 August 2024

Abstract

Stable isotope ratios of nitrate (NO_3^-) can be used as a tool to investigate NO_3^- dynamics in watersheds over the world. However, most of the NO_3^- source analyses from watersheds using isotopes have been conducted during baseflow conditions, and more information is required on conditions during rainfall, which is a crucial period for nitrogen export to downstream ecosystems. Additionally, there is limited information regarding the sources of stable isotopes of NO_3^- in watersheds of Japan. We measured the nitrogen and oxygen isotopes of NO_3^- ($\delta^{15}N–NO_3^-$ and $\delta^{18}O–NO_3^-$) in the Yasu River during baseflow and rainfall events and those from major NO_3^- sources in the watershed. The $\delta^{15}N–NO_3^-$ exported from forests and rice paddies showed small fluctuations, while there were large fluctuations in the $\delta^{15}N–NO_3^-$ exported from sewage treatment plants, suggesting the need to obtain data on $\delta^{15}N–NO_3^-$ exported from sewage treatment plants. The NO_3^- concentrations in the Yasu River during summer baseflow were too low to be explained by the mixing of NO_3^- sources within the watershed, suggesting that NO_3^- consumption processes within the river and groundwater influence the NO_3^- concentrations. Furthermore, the sources of NO_3^- exported from the watershed differed during baseflow and rainfall, with a larger contribution of forest-derived NO_3^- during rainfall. Monitoring during rainfall is therefore essential to determine the sources of NO_3^- exported from the watershed.

Keywords Nitrate · Isotopes · Watershed · Rainfall events

Introduction

In recent decades, nitrogen loading to terrestrial ecosystems has continued to increase globally due to NOx emissions from fossil fuel combustion and ammonia (NH_4^+) and nitrate (NO_3^-) pollutions from chemical fertilizer production (Galloway et al. 2008). Nitrogen compounds exported from terrestrial ecosystems to water bodies, such as lakes and coastal areas, through rivers can lead to eutrophication and greenhouse gas emissions in aquatic ecosystems (Anderson et al. 2002; McCrackin and Elser 2010). Therefore, to manage aquatic environments, it is necessary to elucidate the processes of nitrogen export from terrestrial to aquatic ecosystems on the watershed scale.

Recently, the stable isotope ratios of nitrogen and oxygen in NO_3^- ($\delta^{15}N–NO_3^-$ and $\delta^{18}O–NO_3^-$) have been used to explore the dynamics and origin of NO_3^- in watersheds. The main nitrogen compound transported through watersheds is NO_3^-, and the $\delta^{15}N–NO_3^-$ and $\delta^{18}O–NO_3^-$ values vary depending on the origin, production, and consumption

Communicated by Noboru Okuda.

✉ Ken'ichi Osaka
osaka.k@ses.usp.ac.jp

1 Faculty of Environmental Science, University of Shiga Prefecture, 2500, Hassaka-Cho, Hikone, Shiga 522-8533, Japan

2 Research Institute for Humanity and Nature, Kyoto, Japan

3 Department of Ecosystem Study, School of Environmental Science, University of Shiga Prefecture, Hikone, Shiga, Japan

4 Division of Environmental Dynamics, Graduate School of Environmental Science, University of Shiga Prefecture, Hikone, Shiga, Japan

5 Department of Social Informatics, Graduate School of Informatics, Kyoto University, Kyoto, Kyoto, Japan

6 Interdisciplinary Center for River Basin Environment, University of Yamanashi, Kofu, Yamanashi, Japan

Published online: 01 September 2024

processes of NO_3^- (Kendall et al. 2007). Therefore, $\delta^{15}N–NO_3^-$ and $\delta^{18}O–NO_3^-$ have been used globally to study the origin and dynamics of NO_3^- exported through rivers from watersheds with various NO_3^- sources, such as forests, agricultural land, and urban areas (Nakamura et al. 2011; Ohte et al. 2010; Sugimoto et al. 2019; Tabayashi et al. 2017) as well as the origin and dynamics of NO_3^- in groundwater (Hosono et al. 2013; Nakagawa et al. 2017; Nishikiori et al. 2012; Yoshimoto et al. 2011). Those studies reported a very strong influence of the land use type in watersheds on both the NO_3^- concentration in groundwater and the NO_3^- discharged from the watersheds. NO_3^- concentrations are high in watersheds with larger proportions of urban and agricultural areas, which load large amounts of NO_3^- derived from anthropogenic sources such as sewage treatment plant discharges and agricultural wastewater.

Most studies using $\delta^{15}N–NO_3^-$ and $\delta^{18}O–NO_3^-$ to investigate NO_3^- exported from watersheds through rivers were conducted under base flow conditions. Few studies used $\delta^{15}N–NO_3^-$ and $\delta^{18}O–NO_3^-$ during rainfall to estimate NO_3^- origin exported from watersheds and then compare the results with those obtained under base flow conditions. Studies using $\delta^{15}N–NO_3^-$ and $\delta^{18}O–NO_3$ to investigate NO_3^- origin exported from watersheds through rivers following rainfall events are particularly lacking in Japan. Although each rainfall event occurs during a short period of time, its role in determining the process and amount of NO_3^- export from a watershed must be considered, given that it may increase water flow by an order-of-magnitude higher than base flow. Moreover, many Japanese rivers are located in a mountainous orogenic belt with steep terrain in the Asian monsoon region, which has heavy summer precipitation. The effect of rainfall on annual nitrogen exports may therefore relatively large. For example, in a study of the Yasu and Hino Rivers, which are major rivers flowing into Lake Biwa in Shiga Prefecture, Okubo (2007) reported that 54.3% and 82.7% of annual dissolved nitrogen exports in the Hino River and Yasu River, respectively, occurred during rainfall. Chiwa et al. (2010) calculated annual nitrogen flux in a forested watershed in Japan using the LQ equation and determined that > 80% of the annual inorganic nitrogen flux was exported during rainfall events.

Changes in the amount, intensity, and timing of precipitation attributable to climate change have been observed on a global scale (Trenberth 2011; Westra et al. 2014). In southern Shiga Prefecture, where this study was conducted, annual precipitation and maximum daily precipitation for 2010–2020 were higher than the 50-year averages for the period 1970–2020 (Katsuyama et al. 2021). It is therefore becoming increasingly important to determine the effect of rainfall on nitrogen exports from watersheds.

Studies of NO_3^- dynamics in watersheds using stable isotope ratios require isotopic information related to the NO_3^- sources in watersheds, such as the $\delta^{15}N$ value of NO_3^- in treated sewage waters, agricultural drainages, and forest streams, but few stable isotope ratio measurements are available for NO_3^- sources in Japanese watersheds, and further data are needed. For example, the $\delta^{15}N–NO_3^-$ values in sewage effluent fluctuate widely and may be affected by sewage treatment methods and the associated NO_3^- removal efficiency (Onodera et al. 2021).

In this study, we measured the $\delta^{15}N–NO_3^-$ and $\delta^{18}O–NO_3^-$ values in a forest stream as well as in paddy field drainage and treated sewage. All three are considered to be the major nitrogen sources in the Yasu River watershed in southern Shiga Prefecture. In addition, the $\delta^{15}N–NO_3^-$ and $\delta^{18}O–NO_3^-$ values in river water collected from the Yasu River under baseflow conditions and during rainfall events were measured to determine the origin and dynamics of NO_3^- exported from the watershed and the effect of rainfall events thereon. In previous studies, $\delta^{15}N–NO_3^-$ and $\delta^{18}O–NO_3^-$ in the Yasu River were measured at 19 sites, from upstream to downstream, under baseflow conditions. NO_3^- concentrations and $\delta^{15}N–NO_3^-$ values were shown to be low in the upper reaches of the river and high in the middle and lower reaches, where agricultural (paddy fields) and urban land uses are dominant. These results suggested that the origin of NO_3^- in the middle and lower reaches of the Yasu River is NO_3^- with high $\delta^{15}N–NO_3^-$ values discharged from paddy fields and sewage treatment plants (Ohte et al. 2010).

Methods

Study site

This study was conducted in the Yasu River watershed (watershed area = 387 km^2, river length = 65.25 km), which is the largest tributary system of Lake Biwa in central Japan (Fig. 1). It originates from Mt. Gozaisyo at an elevation of 1213 m and flows out to the lake basin at an elevation of 85 m. The mean annual precipitation and mean annual temperature from 2013 to 2016 at the Tsuchiyama meteorological station (34°56.3′ N, 136°16.7′ E) of the Japan Meteorological Agency (JMA) near the center of the Yasu River watershed were 1644 mm and 13.6 °C, respectively. In the Yasu River, forest accounts for 55.3% of its watershed area, rice paddy 21.6%, urban 11.1%, cropland 2.1%, water body 1.8%, and other 8.2%. Further details of the Yasu River watershed can be found in Ishida et al. (2019) and Osaka et al. (2022).

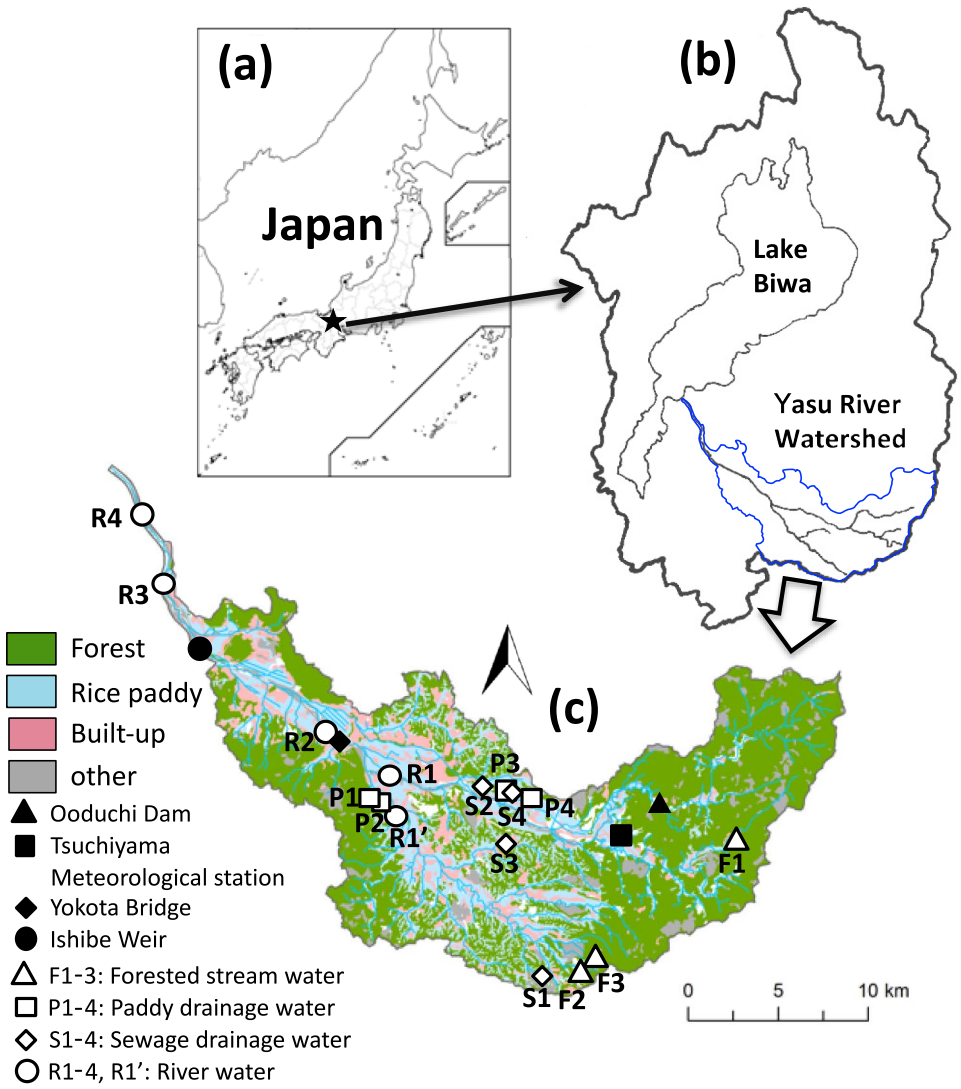

Fig. 1 **a**, **b** Location of the study sites. The blue line in **b** represents the boundary of the Yasu River watershed in Shiga Prefecture, Japan. **c** Map showing land uses in the Yasu River watershed. Solid triangles indicate forested stream water sampling sites, open squares paddy drainage water sampling sites, solid diamonds treated sewage drainage water sampling sites, and open circles river water sampling sites. The solid symbols are the locations where open-access data were collected. The figure was modified from Osaka et al. (2022)

Sampling design

In this study, stream water discharged from forests at three sites (F1–3), drainage water discharged from paddy field areas at four sites (P1–4), treated water discharged from a sewage treatment plant at four sites (S1–4), river water from the mainstream of the Yasu River at three sites (R1, 2, and 4), and river water from the Soma River, a tributary of the Yasu River, at one site (R1') were collected in the Yasu River watershed on 7 June, 17 July, 20 August, 27 September, 30 October, and 29 November, 2018. On 17 July, 20 August, 30 October, and 29 November there were no rainfall events > 4.0 mm within 3 days before sampling, but on 7 June there was 77.5 mm of rainfall just prior to sampling (1:00–6:00 on 7 June), and on 27 September there was 47.0 mm of rainfall just prior to sampling (from 14:00 on 26 September to 8:00 on 27 September). On November 29, there was a weak evening shower at the last sampling point (F2). At the sewage treatment plants, treatment at S1, S3, and S4 consistent of the suspended microorganism method and batch-activated sludge method, while treatment at S2 was by the suspended microorganism method and contact aeration method. The maximum planned volume of sewage treatment for S1, S2, S3, and S4 are 150, 144, 285, and 1,840 m^3/day, respectively. Forested stream water, paddy field drainage, and treated sewage water were collected with a dipper, while river water was collected by dropping a bucket tied with a string from a bridge. Water sampling was conducted once a month from June to November 2018. However, treated sewage and paddy field drainage were sometimes not collected due to the lack of drainage.

In addition to the regular water sampling described above, river water was sampled during rainfall events at R3 (Fig. 1) in the mainstem of the Yasu River on two occasions during this study. A total of 39 river water samples were collected at 2- to 24-h intervals during a rainfall event from 24

to 31 October 2013 (total precipitation 43 mm); 38 samples were collected at 1- to 24-h intervals during a rainfall event from 29 August to 3 September 2016 (total precipitation = 97 mm). Samples were collected using automatic water samplers (models 6712 and 3700; Teledyne ISCO, USA). The collected water samples were placed in polypropylene bottles and returned to the laboratory in refrigerated cooler boxes.

Chemical analysis

Water samples brought back to the laboratory were filtered through a cellulose acetate membrane filter with a pore size of 0.45 µm (C045A047A, ADVANTEC, Japan) on the same day, and the filtrates were frozen in polypropylene bottles at –24 °C. The NO_3^- concentrations were determined by ion chromatography (Integrion; Thermo Fisher Scientific, USA). NO_3^- was reduced to N_2O using a denitrification technique (Casciotti et al. 2002; Sigman et al. 2001), and the nitrogen and oxygen stable isotope ratios of NO_3^- were determined by a gas chromatography combustion isotope ratio mass spectrometry (GC/C/IRMS: Hydra20-20, Sercon, UK) with gas purification and concentration (cryoPREP, Sercon, UK).

Isotope analyses in this study were run simultaneously with the international standards USGS32 ($\delta^{15}N$: 180‰, $\delta^{18}O$: 25.7‰), USGS34 ($\delta^{15}N$: –1.8‰, $\delta^{18}O$: –27.9‰), USGS35 ($\delta^{15}N$: 2.7‰, $\delta^{18}O$: 57.5‰), and IAEA-NO-3 ($\delta^{15}N$: 4.7‰, $\delta^{18}O$: 25.6‰). By analyzing these standards simultaneously with the samples, we calculated the $\delta^{15}N$ and $\delta^{18}O$ values of NO_3^- from the measured $\delta^{15}N$ and $\delta^{18}O$ of N_2O. For $\delta^{18}O$, the values change largely during the reduction of NO_3^- to N_2O (Casciotti et al. 2007), but we could correct this by measuring the international standards described above.

USGS35 is exceptionally high in $\delta^{17}O$ (51.5‰), so a few $^{14}N^{14}N^{17}O$ is formed when it is reduced from NO_3^- to N_2O. Since $^{14}N^{14}N^{17}O$ has the same mass (44) as $^{15}N^{14}N^{16}O$ and $^{14}N^{15}N^{16}O$, the measurement value of $\delta^{15}N$ of USGS35 may be higher than the actual value due to $^{14}N^{14}N^{17}O$ contamination. Therefore, USGS35 was not used for the $\delta^{15}N$ correction. The standard deviations (SDs) with sample size in parenthesis for repeated measurements of $\delta^{15}N$–NO_3^- for the standards USGS32, USGS34, and IAEA-NO-3, which were analyzed repeatedly in this study, were 0.4‰ (28), 0.2‰ (28), and 0.2‰ (26), respectively. The SDs (sample size) for repeated measurements of $\delta^{18}O$–NO_3^- for the standards USGS32, USGS34, USGS35, and IAEA-NO-3 were 0.8‰ (28), 0.7‰ (28), 0.9‰ (26), and 0.6‰ (26), respectively.

Data analysis

We used the median as representative value for each monitoring data set. Each data set was compared using the Dwass-Steel-Critchlow-Fligner (DSCF) test, a nonparametric multiple comparison test, because some of our data sets did not fit a normal distribution. The statistical software jamovi was used for these calculations.

Isotope mixing model

In this study, we used the same simple mixing model as Langmuir et al. (1978) based on NO_3^- concentration and $\delta^{15}N$–NO_3^- in the water [Eqs. (1) and (2)]. Two sources, water A, with a NO_3^- concentration of a mgN/L and a $\delta^{15}N$–NO_3^- value of α‰, and water B, with a NO_3^- concentration of b mgN/L and a $\delta^{15}N$–NO_3^- value of β‰, were mixed at mixing ratio r ($0 \le r \le 1$), where r is the proportion of environmental water A to mixed water C. The NO_3^- concentration c mgN/L and the $\delta^{15}N$–NO_3^- χ‰ of mixed water C can be expressed as shown in Eqs. (1) and (2):

$$c = a\,r + b(1-r) \tag{1}$$

$$\chi = \{\alpha a r + \beta b(1-r)\}/\{a\,r + b(1-r)\} \tag{2}$$

For example, when three different NO_3^- sources (1–3) are mixed as shown in Fig. 2, the NO_3^- concentration and the $\delta^{15}N$–NO_3^- value of the mixture are expected to fall within the mixing lines between two of the three NO_3^- sources.

Public data used in this study

In addition to the data obtained by sampling and chemical analysis, we also used the data on water level monitored at Yokota Bridge, which was publicly available from the Shiga

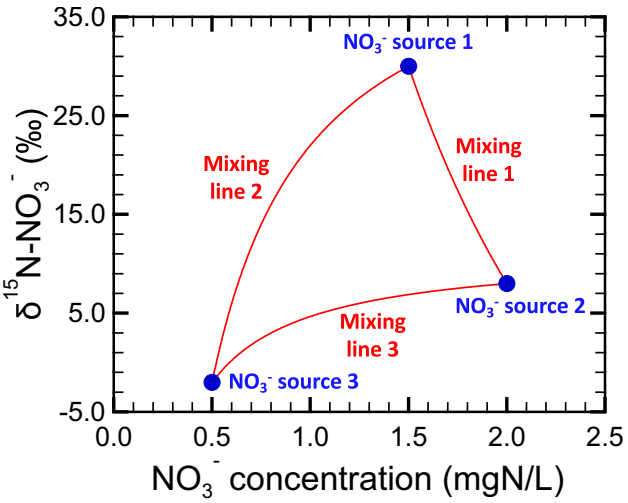

Fig. 2 The isotope mixing model in this study. When three different NO_3^- sources (1–3) are mixed, the NO_3^- concentration and $\delta^{15}N$–NO_3^- of the mixture are expected to fall within mixing lines 1, 2, and 3. The mixing lines can be calculated using Eqs. (1) and (2)

Prefecture through the Civil Engineering Disaster Prevention Information System (Shiga Prefecture 2023). Water quality data were obtained from Ishibe Wier Observatory, being provided by the Ministry of Land, Infrastructure, Transport and Tourism (MLIT) through its Hydrologic and Hydrochemical Quality Database (MLIT 2023a). Rainfall data were obtained from Tsuchiyama Observatory, being published by the JMA via its website (JMA 2023). Discharge data were obtained from Ooduchi Dam, being published by the MLIT on its database of dam discharge (MLIT 2023b).

Results

NO_3^- concentrations and $\delta^{15}N$–NO_3^- and $\delta^{18}O$–NO_3^- values of major NO_3^- sources in the Yasu River watershed

Figure 3 shows the spatial distribution of NO_3^- concentrations, and $\delta^{15}N$–NO_3^- and $\delta^{18}O$–NO_3^- values in the potential sources and river waters in the Yasu River watershed. For forest streams, paddy field drainages, and treated sewage waters, median NO_3^- concentrations were 0.35, 1.15, and 1.77 mgN/L, and their median $\delta^{15}N$–NO_3^-values –0.8, 8.2, and 25.6‰, respectively. The median $\delta^{18}O$–NO_3^- in the forest streams, paddy field drainages, and treated sewage waters were –0.5, 1.2, and 3.1‰, respectively. The NO_3^- concentrations and $\delta^{15}N$–NO_3^- and $\delta^{18}O$–NO_3^- values showed no clear seasonal variations. Multiple comparisons using the Dwass-Steel-Critchlow-Fligner (DSCF) test showed that the NO_3^- concentrations were significantly different between the forest streams and paddy field drainages ($p < 0.01$), and between the forest streams and treated sewage waters ($p < 0.001$). The $\delta^{15}N$–NO_3^- values were significantly different among all nitrogen sources ($p < 0.001$), and the $\delta^{18}O$–NO_3^- values were significantly different between the forest streams and treated sewage waters ($p < 0.05$).

The median NO_3^- concentrations for river waters were 0.39 mgN/L, which was lower than that of paddy field drainages ($p < 0.005$) and treated sewage waters ($p < 0.001$). The median of $\delta^{15}N$–NO_3^- and $\delta^{18}O$–NO_3^- values for river waters were 7.1 and 1.2‰, respectively.

Temporal variation of NO_3^- concentrations and $\delta^{15}N$–NO_3^- and $\delta^{18}O$–NO_3^- values in the Yasu River

Figure 4 shows the temporal variations of NO_3^- concentrations, and the $\delta^{15}N$–NO_3^- and $\delta^{18}O$–NO_3^- values, at sites R1', R1, R2, and R4 in the Yasu River in 2018. On 7 June

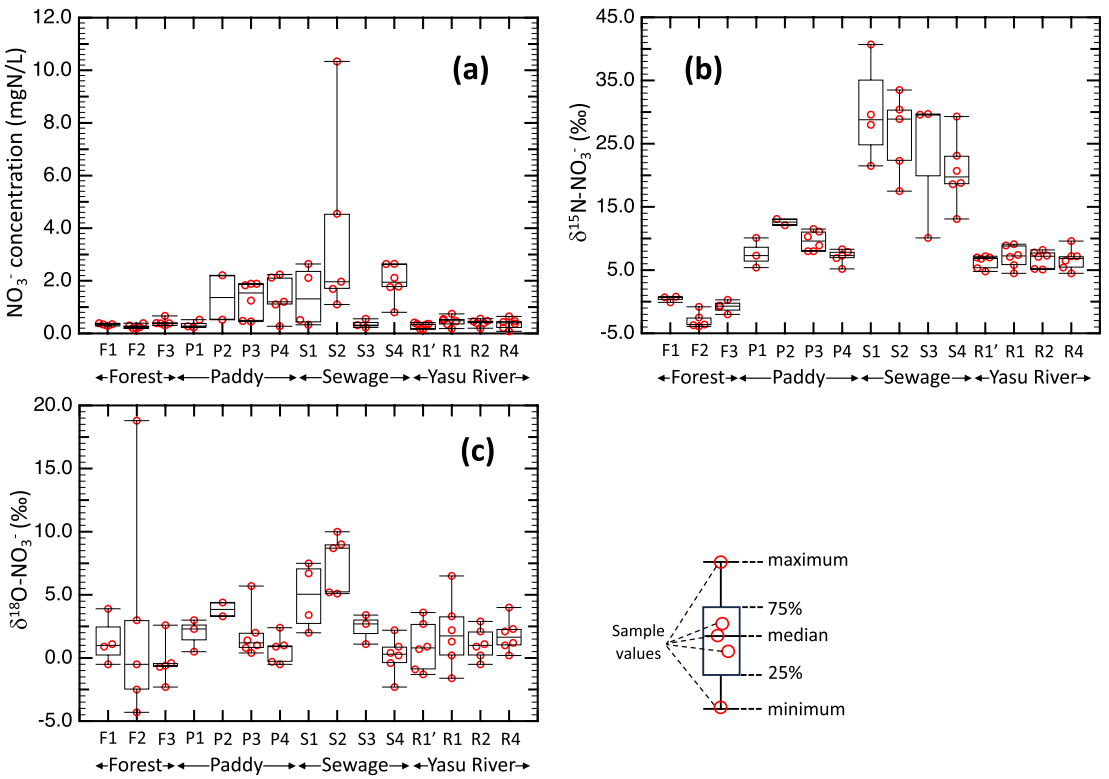

Fig. 3 Spatial distribution of the **a** NO_3^- concentrations, **b** $\delta^{15}N$–NO_3^- values, and **c** $\delta^{18}O$–NO_3^- values in potential NO_3^- sources and river waters in the Yasu River watershed. Red circles are measured values

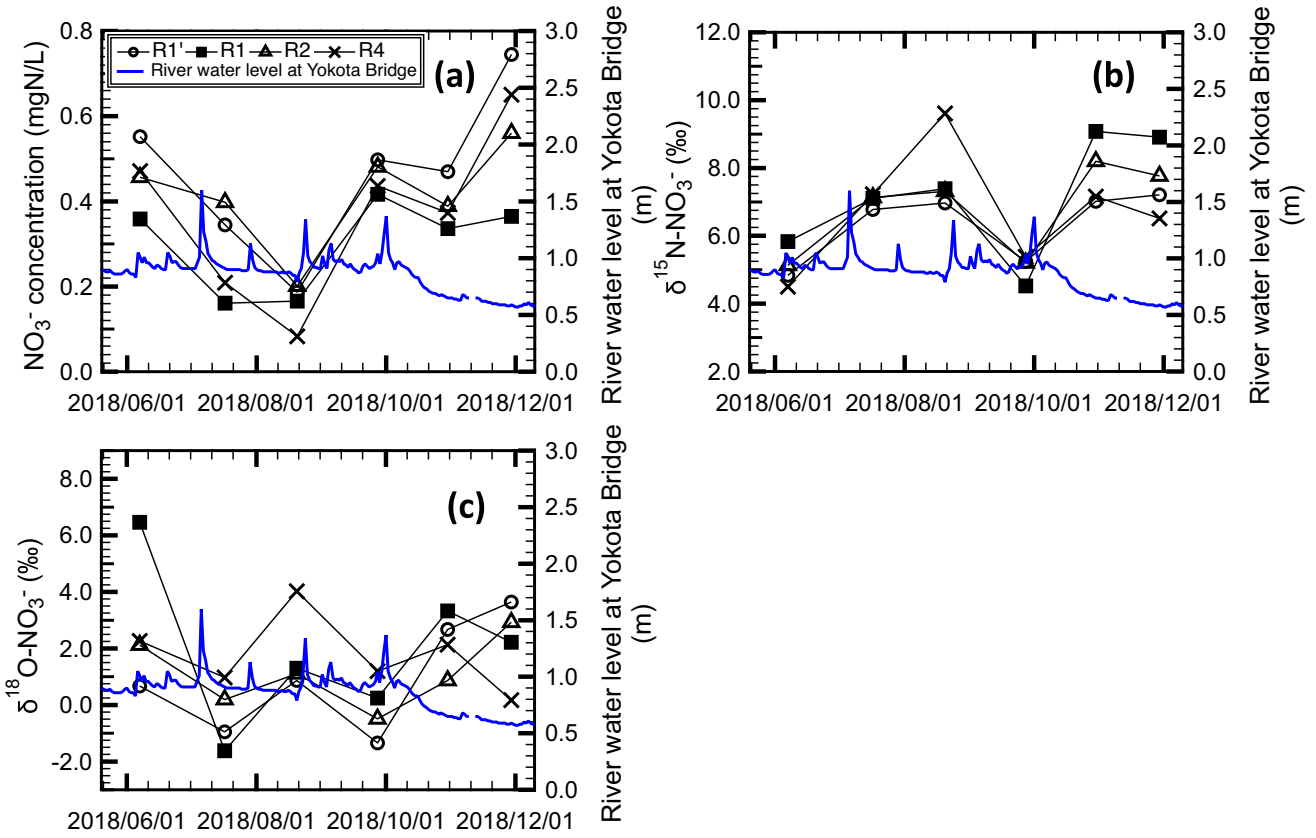

Fig. 4 Temporal variation of the **a** NO_3^- concentration, **b** $\delta^{15}N$–NO_3^- value, and **c** $\delta^{18}O$–NO_3^- value in the Yasu River. The blue line represents the water level at Yokota Bridge

and 27 September, precipitation occurred just before water sampling. The NO_3^- concentrations in the Yasu River were lower from July to August (summer) than in other seasons at all sites. The lowest NO_3^- concentration in August (0.08 mgN/L) was found at the most downstream site, R4. In contrast to the NO_3^- concentrations, there was no clear seasonal variation in the $\delta^{15}N$–NO_3^- values, which were low on 7 June and 27 September, when precipitation occurred immediately before water sampling. On 7 June and 27 September, the median $\delta^{15}N$–NO_3^- values were 5.0 and 5.3‰, respectively, while the median $\delta^{15}N$–NO_3^- value on the other sampling dates was 7.2‰. In contrast to the NO_3^- concentrations, there were no clear seasonal variations in $\delta^{18}O$–NO_3^-. Also, in contrast to $\delta^{15}N$–NO_3^-, $\delta^{18}O$–NO_3^- did not greatly vary even when rainfall occurred immediately before sampling. River water levels dropped sharply after October, but there were no clear relationships among the NO_3^- concentrations, $\delta^{15}N$–NO_3^- values, $\delta^{18}O$–NO_3^- values, and river water levels.

Figure 5 shows the NO_3^- concentrations monitored at Ishibe Wier Observatory in the Yasu River by MLIT from 2013 to 2018, the water discharge from Ooduchi Dam, the water level of the Yasu River at Yokota Bridge monitored by Shiga Prefecture, and the precipitation at Tsuchiyama monitored by the JMA. Lower NO_3^- concentrations in the Yasu River were observed every summer, suggesting that the summer decrease in NO_3^-concentration observed in this study was the seasonal pattern characteristic to the Yasu River.

Fluctuations in the NO_3^- concentrations and $\delta^{15}N$–NO_3^- and $\delta^{18}O$–NO_3^- values in the Yasu River during rainfall

Figure 6 shows the fluctuations of NO_3^- concentrations and $\delta^{15}N$–NO_3^- and $\delta^{18}O$–NO_3^- values during October 2013 and August 2016. During the rainfall event in October 2013, the NO_3^- concentration before the rainfall was 0.87 mgN/L, while the NO_3^- concentration decreased to 0.57 mgN/L as the river discharge rate increased. In August 2016, in contrast, the NO_3^- concentration was 0.26 mgN/L before the rainfall event but it increased to 0.69 mgN/L as the river discharge rate increased. While the fluctuations of the NO_3^- concentrations differed during the studied rainfall events, the $\delta^{15}N$–NO_3^- value followed similar trends, decreasing from 6.4 to 2.3‰ with the increasing river discharge rate during the October 2013 rainfall event and from

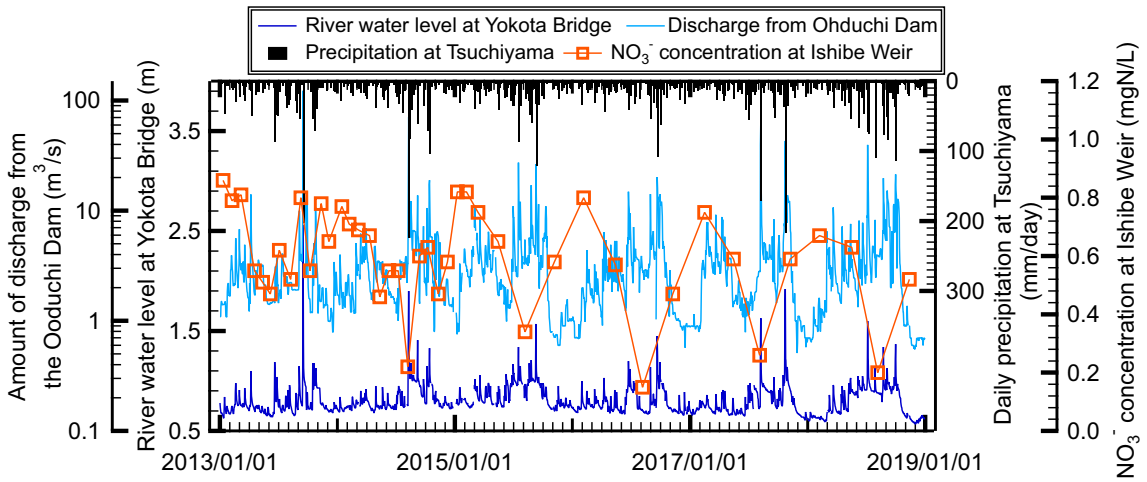

Fig. 5 Precipitation at Tsuchiyama in the Yasu River watershed, water level at Yokota Bridge on the Yasu River, water discharge from Ooduchi Dam (upstream of the Yasu River), and temporal variation of the NO_3^- concentration at Ishibe Wier Observatory in the Yasu River

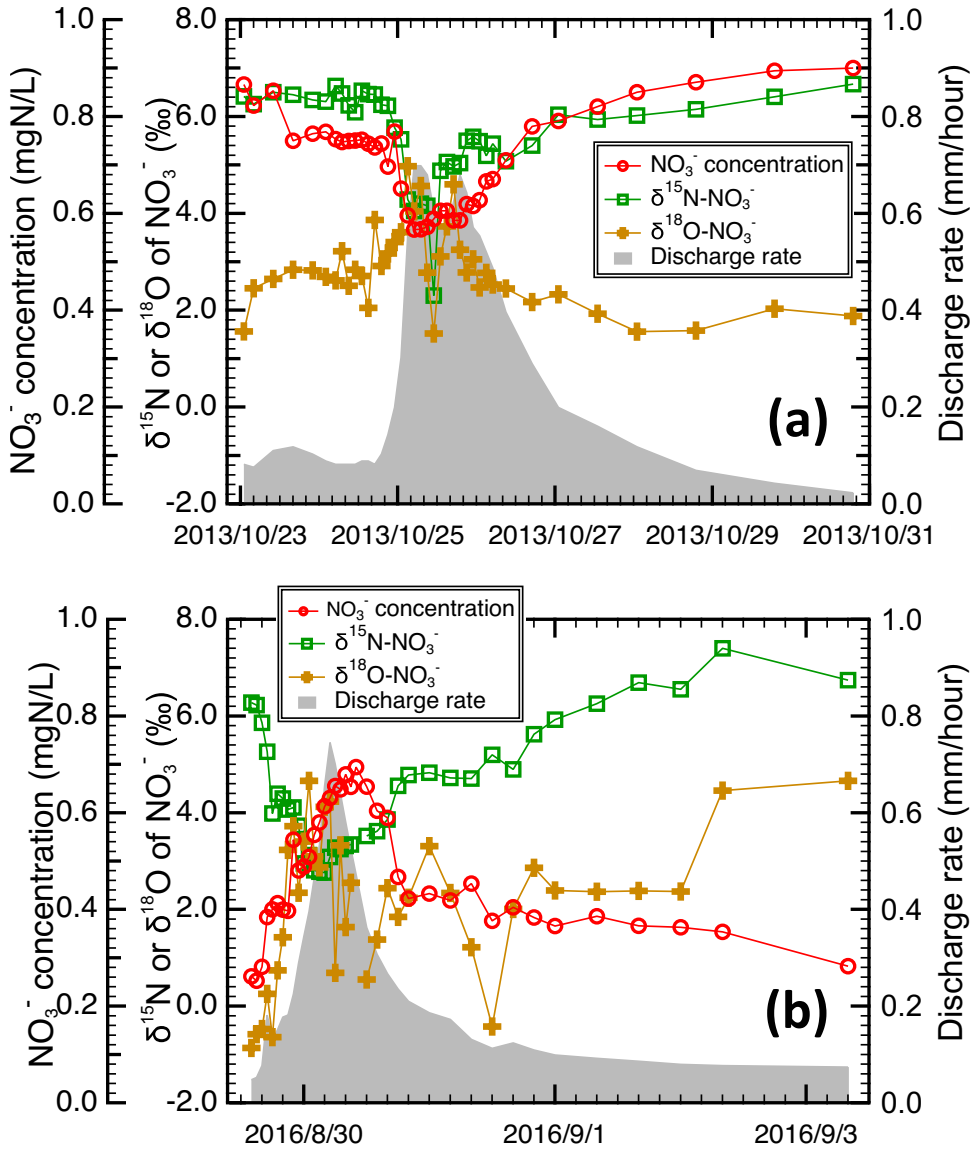

Fig. 6 Temporal variations of NO_3^- concentrations, $\delta^{15}N$–NO_3^- and $\delta^{18}O$–NO_3^- values, and discharge at site R3 in the Yasu River during rainfall events in October 2013 (**a**) and August–September 2016 (**b**)

6.2 to 2.8‰ with the increasing river discharge rate during the August 2016 rainfall event.

Discussion

$\delta^{15}N$ values of the major NO_3^- sources within the Yasu River watershed

The narrow range of variability of the $\delta^{15}N$–NO_3^- values in the forest stream and paddy field drainage measured in this study was similar to previously reported measurements in Japan (Table 1). Compared with previously reported NO_3^- sources in the watershed (e.g., Kendall et al. 2007), NO_3^- in the forest streams in this study may be derived from nitrification in the soil, and the NO_3^- in the paddy field drainages from organic fertilizers. However, weakly positive relationships were found between $\delta^{15}N$–NO_3^- and $\delta^{18}O$–NO_3^- in the forest streams and paddy drainages (Fig. 7). During denitrification, $\delta^{15}N$–NO_3^- and $\delta^{18}O$–NO_3^- values increase simultaneously (Kendall et al. 2007; Osaka et al. 2018), suggesting that denitrification was responsible for the variation in the $\delta^{15}N$–NO_3^- values in the forest streams and paddy field drainages.

The $\delta^{15}N$–NO_3^- values in treated sewage waters were much more variable than those in the forest streams and

Table 1 Nitrogen and oxygen stable isotope ratios of NO_3^- exported from treated sewage waters (a), forest streams (b), and rice paddy fields (c) in Japan

$\delta^{15}N$ (‰)			$\delta^{18}O$ (‰)			References	Note	Site
Average	SD	Range	Average	SD	Range			
(a) Treated sewage waters								
		11.3–17.4				Arai and Tase (1992)	1 sewage treatment plant	Tokyo
18.1		17.1–19.0				Kondo et al. (1997)	2 sewage treatment plants or one sewage treatment plants at twice	Okinawa
19.5	5.5	12.9–29.8				Toda et al. (2002)	Isotopic values of TDN, 6 sewage treatment plants	Nakano
21.87	3.09	18.70–27.09	8.52	4.48	4.4–16.75	Tabayashi et al. (2017)	6 sewage treatment plants	Shimane
14						Saito et al. (2018)	3 sewage treatment plants	Osaka
		7.5–25.5				Onodera et al. (2021)	4 treatments in one treatment plant	
24.7 (25.6)	7.7	10.1–40.7	3.7 (3.1)	3.6	− 2.3–10.0	This study	4 sewage treatment plants	Shiga
(b) Forest streams								
		− 1.2–6.0				Konohira et al. (1997)	Forested watershed with N saturated and well dentrified, rainfall event	Tokyo
− 0.2	2.9	− 4.0–4.6	0.5	1.4	− 1.6–2.8	Tsunogai et al. (2010)	9 forest sites, baseflow	Hokkaido
1.9			2.2			Osaka et al. (2010)	Average of one half year observation at one site, baseflow	Shiga
2.4	1.5	− 1.4–5.1	5.1	7.4	− 7.1–20.3	Tobari et al. (2010)	23 forest sites, baseflow	Wakayama
0.6	1.1	− 1.4–2.5	− 1.1	2.1	− 3.5–3.4	Nakamura et al. (2011)	15 forest sites, baseflow	Yamanashi
1.5	1.0	− 1.0–4.0	− 0.2	3.7	− 8.1–5.7	Tabayashi and Koba (2011)	24 forest sites, abundant N deposition, baseflow	Saitama
− 1.2 (− 0.8)	1.7	− 3.9–0.8	1.3 (− 0.5)	5.5	− 4.3–18.8	This study	3 forest sites, baseflow	Shiga
(c) Rice paddy fields								
8.8						Park et al. (1998)	Surface water at paddy, the value of irrigation water is 8.29–9.13 ‰, High NO_3^- concentration of irrigation water	Saitama
12.3	2.2	9.1–14.1				Toda et al. (1997)	Drainage water, the value of irrigation water is 7.0–7.4 ‰, High NO_3^- concentration of irrigation water	Shizuoka
7.9	2.9					Nguyen et al. (2015)	Drainage water, the value of irrigation water is 6.6 ‰	Yamanashi
8.8 (8.2)	2.3	5.2–13.1	1.8 (1.2)	1.7	− 0.5–5.7	This study	Drainage water	Shiga

In this study, median values were used as representative values of isotope ratios. However, in this table, the average values are included for comparison with previous studies. The numbers in parentheses in the table are median values

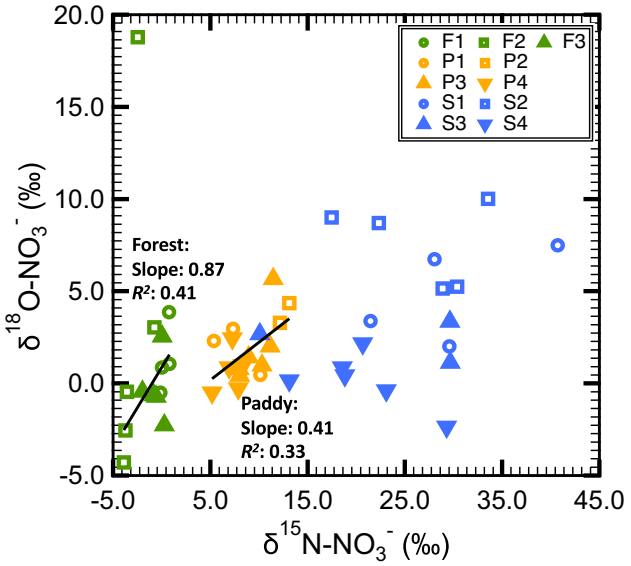

Fig. 7 Relationships between $\delta^{15}N–NO_3^-$ and $\delta^{18}O–NO_3^-$ in forest streams, paddy field drainages, and treated sewage waters. In a forest stream, one sample with a very high $\delta^{18}O–NO_3^-$ value was collected an evening shower event, so that its data were excluded from the regression analysis

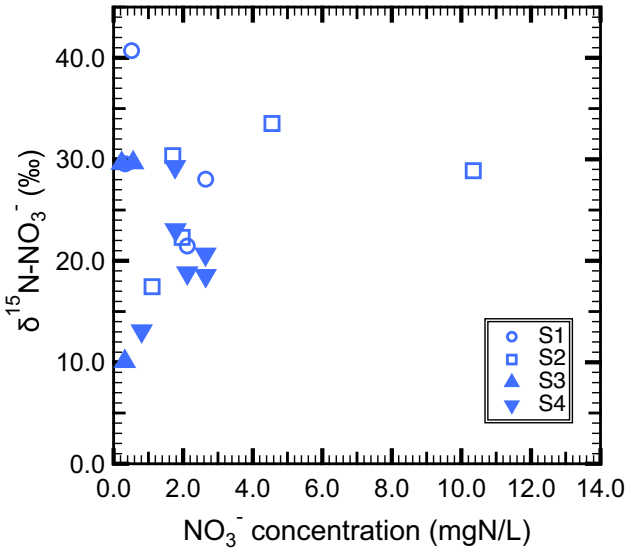

Fig. 8 Relationship between NO_3^- concentrations and $\delta^{15}N–NO_3^-$ in treated sewage waters

paddy field drainages, and their median values were slightly higher than previously reported values (Table 1). Arai and Tase (1992) measured treated sewage water flowing into the Tamagawa Jousui Channel and reported that $\delta^{15}N–NO_3^-$ tended to increase as the NO_3^- concentration in the treated sewage water decreased. Onodera et al. (2021) also reported that in sewage treatment plants where advanced treatment technologies were applied, the $\delta^{15}N–NO_3^-$ and $\delta^{18}O–NO_3^-$ values of wastewater were higher when the NO_3^- removal efficiency was high. These results were considered reasonable because denitrification in the sewage treatment process would lower NO_3^- concentrations in the treated sewage water and increase the $\delta^{15}N–NO_3^-$ value.

However, the results of our study slightly differed from those in the above studies. There was no clear and consistent relationship between NO_3^- concentrations and $\delta^{15}N–NO_3^-$ values in the treated sewage waters (Fig. 8). However, the variations in $\delta^{15}N–NO_3^-$ values were larger in treated sewage waters with low NO_3^- concentrations than in treated sewage waters with high NO_3^- concentrations. NO_3^- generated by nitrification has a lower $\delta^{15}N$ value than the $\delta^{15}N$ value of NH_4^+, the substrate for nitrification (Kendall et al. 2007), and the $\delta^{15}N$ value of NO_3^- produced solely by nitrification is typically lower than the $\delta^{15}N$ value of the environmental NO_3^- pool (e.g., Osaka et al. 2010). One possible reason for the high variation in $\delta^{15}N–NO_3^-$ values in the treated sewage waters with low NO_3^- concentrations in this study is that efficient denitrification occurred during the sewage treatment process, increasing the $\delta^{15}N–NO_3^-$ value. Alternatively, the low NO_3^- concentrations may have been strongly influenced by NO_3^- that was newly produced by nitrification and therefore had relatively low $\delta^{15}N$ values. Consequently, when the NO_3^- concentrations in treated sewage waters were low, the $\delta^{15}N–NO_3^-$ values may have been strongly affected by the balance between NO_3^- production and consumption. The lack of a clear relationship between $\delta^{15}N–NO_3^-$ and $\delta^{18}O–NO_3^-$ in treated sewage waters in this study (Fig. 7) also suggests that NO_3^- source isotope signatures were not solely determined by denitrification. However, further data are necessary to discuss in detail because of lack of data on $\delta^{15}N–NO_3^-$ in treated sewage waters.

NO_3^- sources and temporal variation in the concentration of NO_3^- discharged from the Yasu River watershed under baseflow conditions

From the monthly water sampling results, the $\delta^{15}N–NO_3^-$ values on 7 June and 27 September, when there was rainfall prior to sampling, were lower than those on other days when there was no rainfall prior to sampling (Fig. 4). This suggested that during rainfall, some NO_3^- was exported from sources different from that of the NO_3^- exported under baseflow conditions. The median $\delta^{15}N–NO_3^-$ value on the sampling days without rainfall was 7.2‰, which was similar to the value of $\delta^{15}N–NO_3^-$ in the middle and lower reaches of the Yasu River reported by Ohte et al. (2010). Ohte et al. (2010) found that NO_3^- concentrations and $\delta^{15}N–NO_3^-$ values were low in the upper reaches of the Yasu River, and simultaneously high in the middle and lower reaches, surrounded by more agricultural land (paddy fields) and urban

areas. This indicated that the NO_3^- in the middle and lower reaches of the Yasu River originated from rice paddies and treated sewage waters with high $\delta^{15}N–NO_3^-$ values. The $\delta^{15}N–NO_3^-$ values in the Yasu River under baseflow conditions in this study were similar to those reported by Ohte et al. (2010), implying that the NO_3^- sources under baseflow conditions were mainly paddy fields and treated sewage waters. In addition, the $\delta^{18}O–NO_3^-$ value in the Yasu River under baseflow conditions was much lower than that from atmospheric deposition (Fig. 4), which ranged from 47.0‰ to 86.5‰ with the average of 71.4‰, measured at Ab-S, the forest site in the Yasu River watershed (Osaka et al. 2016). Therefore, the contribution of atmospheric deposition to the NO_3^- discharge from the Yasu River under baseflow conditions was not considered significant.

The NO_3^- concentration in the Yasu River under baseflow conditions tended to vary depending on the season, with lower concentrations in summer than in the other seasons (Fig. 4). To elucidate the process responsible for the seasonal variation in NO_3^- concentrations, as

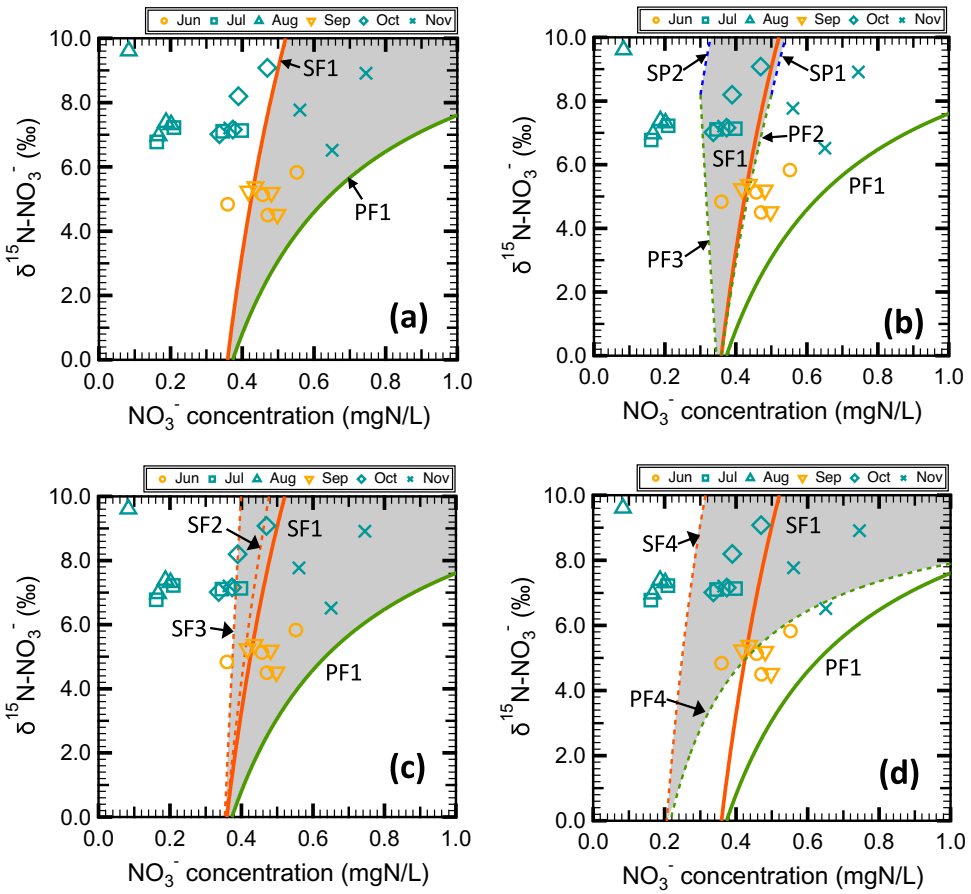

Fig. 9 Relationships between the NO_3^- concentration and $\delta^{15}N–NO_3^-$ value in Yasu River at monthly sampling. Yellow symbols indicate samples from sites where rainfall occurred immediately prior to water sampling. Blue symbols indicate samples taken under baseflow conditions. The orange line shows a relationship between the NO_3^- concentration and $\delta^{15}N–NO_3^-$ value when the treated sewage water and forest stream are mixed. The green line shows a relationship between the NO_3^- concentration and $\delta^{15}N–NO_3^-$ value when the paddy field drainage and forested stream water are mixed. The blue line shows the relationship between the NO_3^- concentration and $\delta^{15}N–NO_3^-$ value when paddy field drainage and treated sewage water are mixed. However, since both paddy field drainages and treated sewage waters have high NO_3^- concentrations and $\delta^{15}N–NO_3^-$, the blue line is outside the range of the figures, except for the panel b. The solid lines (SF1 and PF1) are the value calculated from the median NO_3^- concentration and $\delta^{15}N–NO_3^-$ value of treated sewage waters, paddy field drainages, and forested stream waters obtained in this study. The dotted lines (SF2–4, PF2–3, and SP1, 2) are the values calculated assuming that treated sewage waters, paddy field drainages, and forested stream waters have lower NO_3^- concentrations than those obtained in this study. Each line was calculated using the parameters in Table 2, using Eqs. (1) and (2). **a** The line calculated from the median NO_3^- and $\delta^{15}N–NO_3^-$ concentrations of forest water, treated sewage water, and paddy drainage. **b** Mixing lines assuming lower NO_3^- concentrations in paddy drainages than our observations. **c** Mixing lines assuming lower NO_3^- concentrations in treated sewage waters than our observations. **d** T Mixing lines assuming lower NO_3^- concentrations in forest streams than our observations. If forest water, treated sewage water, and paddy drainage are mixed according to **a**–**d**, the NO_3^- concentrations and $\delta^{15}N–NO_3^-$ values of the water after mixing would fall within the gray area

shown in Fig. 9a, the median NO_3^- concentrations and $\delta^{15}N–NO_3^-$ values determined for the forest stream, paddy drainage, and treated sewage water were used to calculate the possible range of NO_3^- concentrations and $\delta^{15}N–NO_3^-$ values in a mixture of these NO_3^- sources. The results showed that the NO_3^- concentrations in the Yasu River, especially during the summer months, are lower than when forest stream water, agricultural drainage, and treated sewage water are mixed together. The solid orange line in Fig. 9a shows the relationship between the NO_3^- concentration and $\delta^{15}N–NO_3^-$ value obtained in a mixture of forested streams and treated sewage water, as determined from the respective median NO_3^- concentrations and $\delta^{15}N–NO_3^-$ values. Similarly, the solid green line in Fig. 9a shows the relationship between the NO_3^- concentration and $\delta^{15}N–NO_3^-$ value following the mixing of forested stream water and paddy field drainage, as determined from the respective median NO_3^- concentrations and $\delta^{15}N–NO_3^-$ values. Therefore, assuming that the concentrations and $\delta^{15}N$ of NO_3^- exported from the Yasu River reflected a mixture of NO_3^- exported from the forested stream, paddy field drainage, and treated sewage water, the values in the Yasu River were in the gray area between the solid orange and green lines of Fig. 9a. However, especially in summer, NO_3^- concentrations were low in the Yasu River under baseflow conditions and were outside the area between those lines (Fig. 9a).

The possible reasons for this are as follows: (i) the actual concentrations of NO_3^- exported from each NO_3^- source in the Yasu River watershed during the summer months were lower than the median NO_3^- concentrations in a forest streams, paddy field drainages, and treated sewage waters determined in this study; (ii) NO_3^- was consumed in the Yasu River (e.g., NO_3^- uptake by attached algae and bacteria and denitrification); and (iii) dilution by groundwater with reduced NO_3^- concentrations due to denitrification and microbial uptake. To test the first possibility, the mixing model in Fig. 9a was recalculated at NO_3^- concentrations lower than the median NO_3^- concentrations measured in the forested stream waters, paddy drainages, and treated sewage waters, as shown in Fig. 9b–d. Figure 9b shows the median NO_3^- concentrations calculated based on a change from 1.16 mgN/L (PF1) to 0.50 mgN/L (PF2 and SP1) and 0.30 mgN/L (PF3 and SP2) in the paddy field drainage. Figure 9c shows the median NO_3^- concentrations calculated based on a change from 2.12 mgN/L (SF1) to 1.00 mgN/L (SF2) and 0.50 mgN/L (SF3) in the treated sewage water. Figure 9d shows the median NO_3^- concentrations calculated based on a change from 0.35 mgN/L (PF1 and SF1) to 0.20 mgN/L (PF4 and SF4) in forested stream water. The results show that the simple mixing model does not explain the low summer NO_3^- concentrations in the Yasu River, even assuming NO_3^- concentrations much lower than the median NO_3^- concentrations in the forested streams, paddy field drainages, and treated sewage waters measured in this study.

Therefore, the low summer NO_3^- concentrations in the Yasu River were most likely due to NO_3^- consumption (e.g., NO_3^- uptake by attached algae and bacteria and denitrification) in the Yasu River or dilution by groundwater with a reduced NO_3^- concentration due to denitrification and microbial uptake. In other words, NO_3^- exported from the Yasu River watershed may be more strongly influenced by NO_3^- consumption in rivers and groundwater under the baseflow condition in summer than in other seasons. The lowest NO_3^- concentrations and highest $\delta^{15}N–NO_3^-$ values were found in the most downstream sample site (R4) in August, when Yasu River NO_3^- concentrations were lowest (Fig. 4); this can be explained by NO_3^- consumption and associated isotopic fractionation during NO_3^- export processes.

The decrease in NO_3^- concentrations during the summer months was not limited to 2018, when our study was conducted, but occurs in most years in the Yasu River (Fig. 5). During the summer, water temperatures and solar radiation are high. This is thought to explain why algae and microbes in the river water are more active, and NO_3^- removal during the river discharge process is more intense than in other seasons. The relative contributions of NO_3^- consumption in the river and in groundwater need to be clarified in future studies.

The sources of NO_3^- exported from the Yasu River watershed during rainfall events

In the two rainfall events that occurred during the different seasons in this study, the NO_3^- concentrations differed in their temporal trends, while $\delta^{15}N–NO_3^-$ values followed a similar trend (Fig. 6). These results suggested that the sources of NO_3^- exported from the watershed differed between baseflow water and rainfall events in both summer and autumn, resulting in seasonal variation in the concentration of NO_3^- exported from the Yasu River. During the October 2013 rainfall event, the NO_3^- concentration decreased to 0.57 mgN/L and the $\delta^{15}N–NO_3^-$ value to 2.3‰ as the river discharge increased (Fig. 6), suggesting that water with lower NO_3^- concentrations and $\delta^{15}N–NO_3^-$ values contributed to Yasu River water (blue area in Fig. 10). In constant, the NO_3^- concentration increased to 0.69 mgN/L and the $\delta^{15}N–NO_3^-$ concentration decreased to 2.8‰ during a rainfall event in August 2016 (Fig. 6), suggesting that water with NO_3^- concentrations > 0.69 mgN/L and $\delta^{15}N–NO_3^-$ values < 2.8‰ contributed to the Yasu River (yellow area in Fig. 10). The $\delta^{18}O–NO_3^-$ value was lower than the value of NO_3^- attributed to atmospheric deposition (average: 71.4‰; Osaka et al. 2016) during the rainfall events in October 2013 and August 2016, such that the contribution of NO_3^- from

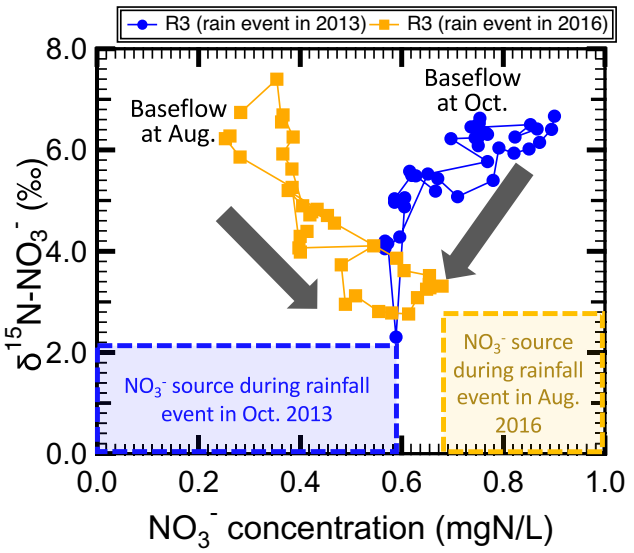

Fig. 10 Relationship between NO_3^- concentrations and $\delta^{15}N$–NO_3^- values during rainfall events at site R3 in the Yasu River. Blue plots are data for October 2013, and yellow data for August 2016. Gray arrows represent the time sequence from the start of the rainfall to the peak flow. Blue square area shows the range of NO_3^- concentrations and $\delta^{15}N$–NO_3^- values of sources that may have flowed into the river water during the increased flow of the October 2013 rainfall event. Yellow square area shows the range of NO_3^- concentrations and $\delta^{15}N$–NO_3^- values for sources that may have flowed into the river water during the August 2016 rainfall flow

atmospheric deposition to NO_3^- export from the Yasu River during these two rainfall events was considered very small.

The median $\delta^{15}N$ values of NO_3^- from the major nitrogen sources in the Yasu River watershed was –0.8‰ in the forest stream, 8.2‰in paddy field drainage, and 25.6‰ in treated sewage water (Fig. 3; Table 1). Assuming that the $\delta^{15}N$ value of NO_3^- exported from each nitrogen source does not vary significantly between baseflow and rainfall events, the $\delta^{15}N$ values of NO_3^- exported from the watershed during rainfall would have been lower than that of treated sewage water and paddy field drainage, suggesting an increased contribution of NO_3^- from the forest stream to the NO_3^- exported from this watershed during rainfall. The median NO_3^- concentration in the studied forest streams under baseflow conditions was 0.35 mg/L and the peak NO_3^- concentrations during the rainfall in 2016 was 0.69 mgN/L. In addition, NO_3^- concentrations were always higher than 0.57 mgN/L during rainfall in 2013. This suggests that forest-derived NO_3^- with a low $\delta^{15}N$ is exported at higher concentrations during rainfall than under baseflow conditions.

NO_3^- concentrations in forested streams during rainfall events are characterized by complex temporal pattern, in which NO_3^- concentrations increase in some cases and decrease in other cases depending on the timing of rainfall (Creed and Band 1998; Katsuyama et al. 1998; Muraoka and Hirata 1988; Osaka et al. 2016; Shinomiya et al. 2006; Yamada et al. 1999). In a forested watershed in the upper Yasu River basin, for example, Osaka et al. (2016) found that the NO_3^- concentrations in stream water over 6 years were within the range of 0.08–1.68 mgN/L, including during rainfall events with a tendency of higher NO_3^- concentrations. Katsuyama et al. (1998) conducted three rainfall studies during summer rainfall and reported that NO_3^- concentrations increased during some rainfall events and decreased during others. These studies included a detailed analysis of the NO_3^- exported from forested watersheds and a high temporal resolution, but they focused on relatively small watersheds and thus had a high spatial heterogeneity. The higher NO_3^- concentrations during rainfall than under baseflow conditions in a forest stream of the large watershed investigated in this study imply that forest NO_3^- export responses to rainfall vary among forests but, on average, NO_3^- concentrations in forested streams increase during rainfall.

In Japan, which has an Asian monsoon climate, summer rainfall has a higher nitrogen export per unit water discharge rate than rainfall of a similar magnitude in other seasons because of the higher NO_3^- production rate by nitrification in the soil during the hot and wet summer months (Osaka et al. 2023; Shinomiya et al. 2006). The higher forest-derived NO_3^- concentrations during August rainfall than during October rainfall, as found in this study, are consistent with the previous findings. The difference in variability of the NO_3^- concentration between the two rainfall events in this study may have been due to the higher concentrations of NO_3^- exported from the forest during the August rainfall event than during the October rainfall event. This finding suggest that such a trend is not limited to the small watersheds reported by Osaka et al. (2023) and Shinomiya et al. (2006) and is also possibly to many other forests.

Conclusions

Stable isotope ratios of NO_3^- are a powerful tool for investigating NO_3^- dynamics in watersheds. This is mainly due to the different $\delta^{15}N$ values among potential NO_3^- sources in watersheds, but there is limited information regarding the $\delta^{15}N$ values of NO_3^- sources in Japanese watersheds. Additionally, most of studies on NO_3^- sources in the watersheds of the world as well as of Japan, using $\delta^{15}N$ have been conducted under baseflow conditions. The source information is also needed during rainfall, which is a crucial event for nitrogen exports to the downstream ecosystem.

In this study, we measured $\delta^{15}N$–NO_3^- exported from forests, paddy fields, and sewage treatment plants, which are major sources of NO_3^- in Japanese watersheds, and compared with the previous data reported in Japan. The $\delta^{15}N$ values of NO_3^- exported from forests and rice

Table 2 The parameters calculated for each mixing line in Fig. 9

Figure panel	Paddy-forest mixing line					Sewage-forest mixing line					Sewage-paddy mixing line				
	Paddy water			Forest water			Sewage water		Forest water			Sewage water		Paddy water	
	Line	NO_3^- conc (mgN/L)	$\delta^{15}N$–NO_3^- (‰)	NO_3^- conc (mgN/L)	$\delta^{15}N$–NO_3^- (‰)	Line	NO_3^- conc (mgN/L)	$\delta^{15}N$–NO_3^- (‰)	NO_3^- conc (mgN/L)	$\delta^{15}N$–NO_3^- (‰)	Line	NO_3^- conc (mgN/L)	$\delta^{15}N$–NO_3^- (‰)	NO_3^- conc (mgN/L)	$\delta^{15}N$–NO_3^- (‰)
a	PF1	1.15	8.2	0.35	− 0.8	SF1	1.77	25.6	0.35	− 0.8					
b	PF1	1.15	8.2	0.35	− 0.8	SF1	1.77	25.6	0.35	− 0.8	SP1	1.77	25.6	0.50	8.2
	PF2	0.50	8.2	0.35	− 0.8						SP2	1.77	25.6	0.30	8.2
	PF3	0.30	8.2	0.35	− 0.8										
c	PF1	1.15	8.2	0.35	− 0.8	SF1	1.77	25.6	0.35	− 0.8					
						SF2	1.00	25.6	0.35	− 0.8					
						SF3	0.50	25.6	0.35	− 0.8					
d	PF1	1.15	8.2	0.35	− 0.8	SF1	1.77	25.6	0.35	− 0.8					
	PF4	1.15	8.2	0.20	− 0.8	SF4	1.77	25.6	0.20	− 0.8					

paddies in this watershed were similar to those in the literature, and their fluctuations were small. Compared to these data, the range of $\delta^{15}N$–NO_3^- values in treated sewage waters was large, especially when the NO_3^- concentration was low. NO_3^- from treated sewage water has a much higher $\delta^{15}N$–NO_3^- value than NO_3^- from other sources in the watershed, which is essential information for identifying the sources of NO_3^- exported from the watershed.

The NO_3^- concentrations in the Yasu River under summer baseflow condition were lower than those for the mixed NO_3^- sources within the watershed, suggesting that NO_3^- consumption processes in river and groundwater reduced the concentrations. As shown in this study, in-river processes may have an important impact on NO_3^- concentrations in river water under baseflow conditions in Japan, but further research is needed.

The sources of NO_3^- exported from this watershed during rainfall events differed from those under baseflow conditions, and the contribution of NO_3^- exported from the forest was greater during rainfall events than under baseflow conditions. In our study, NO_3^- concentrations in the forested stream water during summer rainfall events were higher than those in forested stream water during rainfall in other seasons, consistent with previous studies in small watersheds in monsoon Asia. During rainfall events, river water discharge increases substantially, and the amount of NO_3^- discharged downstream is higher than under baseflow conditions. The fact that, in this study, NO_3^- sources and its export processes in the watershed differed between baseflow and rainfall events stresses the importance of intensive monitoring during rainfall events to understand the processes of NO_3^- export from the watershed.

Acknowledgements We gratefully acknowledge the support and suggestions of members of our laboratory at the University of Shiga Prefecture and Interdisciplinary Center for River Basin Environment (ICRE), University of Yamanashi. We also gratefully acknowledge the support and suggestions of members of the "Towards Sustainable Nitrogen Use Connecting Human Society and Nature" Project, Research Institute for Humanity and Nature (RIHN, a constituent member of NIHU, Project No. 14210156). This research was supported in part by a JSPS Grant-in-Aid (20H04311).

Author contributions KO and MT substantially contributed to the study conception. KO, MT, TI and SC conducted field sampling. KO, MT, TI, SC, and TN performed chemical and isotopic analysis. KO, MT, TI, SC, and TN discussed the results. KO and MT wrote the first draft of the manuscript. All authors contributed to manuscript drafting.

Data availability Data are available from the authors upon reasonable request.

Declarations

Conflict of interest The authors have no competing interests to declare that are relevant to the content of this article.

References

Anderson DM, Glibert PM, Burkholder JM (2002) Harmful algal blooms and eutrophication: nutrient sources, composition and consequences. Estuaries 25(4b):704–726. https://doi.org/10.1007/BF02804901

Arai H, Tase N (1992) Evaluation of self-purification in Tamagawa Jousui channel by using ^{15}N natural isotope (in Japanese). Environ Sci 5(4):249–258. https://doi.org/10.11353/sesj1988.5.249

Casciotti KL, Sigman DM, Hastings MG, Böhlke JK, Hilkert A (2002) Measurement of the oxygen isotopic composition of nitrate in seawater and freshwater using the denitrifier method. Anal Chem 74:4905–4921. https://doi.org/10.1021/ac020113w

Casciotti KL, Böhlke JK, McIlvin MR, Mroczkowski SJ, Hannon JE (2007) Oxygen isotopes in nitrite: analysis, calibration, and equilibration. Anal Chem 79:2427–2436. https://doi.org/10.1021/ac061598h

Chiwa M, Maruno R, Ide J, Miyano T, Higashi N, Otsuki K (2010) Role of stormflow in reducing N retention in a suburban forested watershed, western Japan. J Geophys Res 115:G02004. https://doi.org/10.1029/2009JG000944

Creed IF, Band LE (1998) Export of nitrogen from catchments within a temperate forest: evidence for a unifying mechanism regulated by variable source area dynamics. Water Resour Res 34:3105–3120. https://doi.org/10.1029/98WR01924

Galloway JN, Townsend AR, Erisman JW, Bekunda M, Cai Z, Freney JR, Martinelli LA, Seitzinger SP, Sutton MA (2008) Transformation of the nitrogen cycle: recent trends, questions, and potential solutions. Science 320:889–892. https://doi.org/10.1126/science.1136674

Hosono T, Tokunaga T, Kagabu M, Nakata H, Orishikida T, Lin IT, Shimada J (2013) The use of $\delta^{15}N$ and $\delta^{18}O$ tracers with an understanding of groundwater flow dynamics for evaluating the origins and attenuation mechanisms of nitrate pollution. Water Res 47:2661–2675. https://doi.org/10.1016/j.watres.2013.02.020

Ishida T, Uehara Y, Iwata T, Cid-Andres AP, Asano S, Ikeya T, Osaka K, Ide J, Privaldos O, Jesus I, Peralta M, E, Triño E, Ko CY, Paytan A, Tayasu I, Okuda N (2019) Identification of phosphorus sources in a watershed using a phosphate oxygen isoscape approach. Environ Sci Technol 53:4707–4716. https://doi.org/10.1021/acs.est.8b05837

JMA (2023) Rainfall data (in Japanese). Available via https://www.data.jma.go.jp/stats/etrn/index.php. Accessed Cited 30 July 2023

Katsuyama M, Ohte N, Asano Y, Kobashi S (1998) The influence of a rainfall event on the chemical changes of forest runoff water (in Japanese with English abstract). Bull Kyoto Univer for 69:26–37

Katsuyama K, Ohte N, Kosugi Y, Tani M (2021) The Kiryu Experimental Watershed: 50-years of rainfall-runoff data for a forest catchment in central Japan. Hydrol Process 35:e14104. https://doi.org/10.1002/hyp.14104

Kendall C, Elliott EM, Wankel SD (2007) Tracing anthropogenic inputs of nitrogen to ecosystems. In: Michener R, Lajtha K (eds) Stable isotopes in ecology and environmental science. Blackwell, Oxford, pp 375–449

Kondo H, Tase N, Hirata T (1997) Nitrogen isotope ratio of ni- trate of groundwater in Miyako Island Okinawa Prefecture (in Japanese with English abstract). J Groundw Hydrol 39:1–15. https://doi.org/10.5917/jagh1987.39.1

Konohira E, Yoh M, Yagi K, Kubota J (1997) Variation in the natural abundance of ^{15}N of NO_3^-N in streamwater during a rainfall event (in Japanese with English abstract). J Jpn Soc Hydrol Water Resour 10:360–366. https://doi.org/10.3178/jjshwr.10.360

Langmuir CH, Vocke RD, Hanson GN, Hart SR (1978) A general mixing equation with applications to Icelandic basalts. Earth Planet Sci Lett 37:380–392. https://doi.org/10.1016/0012-821X(78)90053-5

McCrackin ML, Elser JJ (2010) Atmospheric nitrogen deposition influences denitrification and nitrous oxide production in lakes. Ecology 91:528–539. https://doi.org/10.1890/08-2210.1

MLIT (2023a) Hydrologic and hydrochemical quality database (in Japanese). http://www1.river.go.jp. Accessed 30 July 2023

MLIT (2023b) Database of dam discharge (in Japanese). https://mudam.nilim.go.jp/chronology/summary/353. Accessed 30 July 2023

Muraoka K, Hirata T (1988) Streamwater chemistry during rainfall events in a forest basin. J Hydrol 102:235–253. https://doi.org/10.1016/0022-1694(88)90100-X

Nakagawa K, Amano H, Takao Y, Hosono T, Berndtsson R (2017) On the use of coprostanol to identify source of nitrate pollution in groundwater. J Hydrol 550:663–668. https://doi.org/10.1016/j.jhydrol.2017.05.038

Nakamura T, Osaka K, Hiraga Y, Kazama F (2011) Nitrogen and oxygen isotope composition of nitrate in streamwater of Fuji River basin (in Japanese with English abstract). J Jpn Assoc Hydrol Sci 41:79–89. https://doi.org/10.4145/jahs.41.79

Nguyen TPM, Nakamura T, Shindo J, Nishida K (2015) Application of stable isotopes to identify nitrogen sources in the outflow waters from paddy. J Water Environ Technol 13:371–381. https://doi.org/10.2965/jwet.2015.371

Nishikiori T, Takamatsu T, Kohzu A, Nakajima Y, Watanabe M (2012) Distribution of nitrate in groundwater affected by the presence of an aquitard at an agricultural area in Chiba, Japan. Environ Earth Sci 67:1531–1545. https://doi.org/10.1007/s12665-012-1598-y

Ohte N, Tayasu I, Kohzu A, Yoshimizu C, Osaka K, Makabe A, Koba K, Yoshida N, Nagata T (2010) Spatial distribution of nitrate sources of rivers in the Lake Biwa watershed, Japan: controlling factors revealed by nitrogen and oxygen isotope values. Water Resour Res 48:1–16. https://doi.org/10.1029/2009WR007871

Okubo T (2007) Quantitative determination of the nutrient flux from the watershed of the Yasu River and the watershed of theHino River, including the rainfall event (in Japanese). Report for the River Foundation research grant

Onodera T, Komatsu K, Kohzu A, Kanaya G, Mizuochi M, Syutsubo K (2021) Evaluation of stable isotope ratios ($\delta^{15}N$ and $\delta^{18}O$) of nitrate in advanced sewage treatment processes: Isotopic signature in four process types. Sci Total Environ 762:144120. https://doi.org/10.1016/j.scitotenv.2020.144120

Osaka K, Ohte N, Koba K, Yoshimizu C, Katsuyama M, Tani M, Tayasu I, Nagata T (2010) Hydrological influences on spatiotemporal variations of $\delta^{15}N$ and $\delta^{18}O$ of nitrate in a forested headwater catchment in central Japan: denitrification plays a critical role in groundwater. J Geophys Res 115:G02021. https://doi.org/10.1029/2009JG000977

Osaka K, Kugo T, Komaki N, Nakamura T, Nishida K, Nagafuchi O (2016) Atmospheric nitrate leached from small forested watersheds during rainfall events: Processes and quantitative evaluation. J Geophys Res 121:2030–2048. https://doi.org/10.1002/2015JG003210

Osaka K, Nakajima Y, Suzuki K, Eguchi S, Katou H (2018) Nitrogen and oxygen isotope enrichment factors of nitrate at different denitrification rates in an agricultural soil. Soil Sci Plant Nutr 64:558–565. https://doi.org/10.1080/00380768.2018.1504321

Osaka K, Chishiro S, Matsumoto Y, Iwata T, Okuda N (2022) Hydrological control of the chemical characteristics of suspended particulate phosphorus in the Yasu River watershed, Japan: Implications for its source and bioavailability. Hydrol Process 36:e14734. https://doi.org/10.1002/hyp.14734

Osaka K, Kunimatsu T, Hida Y, Komai Y, Katsuyama M, Ohte N (2023) Hydrological and biogeochemical controls of the seasonality of particulate and dissolved nitrogen exports during rainfall

events from a forested watershed in monsoon Asia. Japan. Water Resour Res 59:e2023WR034756. https://doi.org/10.1029/2023WR034756

Park KL, Hidaka S, Kumazawa K (1998) Concentration of nitrate nitrogen and its $\delta^{15}N$ value in the surface water of a paddy field irrigated with spring water from the Kushibiki plateau in Saitama prefecture (in Japanese with English abstract). Jpn J Soil Sci Plant Nutr 69:287–292. https://doi.org/10.20710/dojo.69.3_287

Shiga Prefecture (2023) Civil engineering disaster prevention information system (in Japanese). https://shiga-bousai.jp/index.php. Acceseed 30 July 2023

Saito M, Onodera S-I, Jin G, Shimizu Y, Taniguchi M (2018) Nitrogen dynamics in a highly urbanized coastal area of western Japan: Impact of sewage-derived loads. Prog Earth Planet Sci. https://doi.org/10.1186/s40645-018-0177-6

Shinomiya Y, Yamada T, Inagaki Y, Torii A (2006) Characteristics of output of NO3-N load during storms in a mountainous headwater catchment of Shimanto River (in Japanese with English abstract). J Jpn Soc Water Environ 11:723–729. https://doi.org/10.2965/jswe.29.723

Sigman DM, Casciotti KL, Andreani M, Barford C, Galanter M, Böhlke JK (2001) A bacterial method for the nitrogen isotopic analysis of nitrate in seawater and freshwater. Anal Chem 73:4145–4153. https://doi.org/10.1021/ac010088e

Sugimoto R, Tsuboi T, Fujita MS (2019) Comprehensive and quantitative assessment of nitrate dynamics in two contrasting forested basins along the Sea of Japan using dual isotopes of nitrate. Sci Total Environ 687:667–678. https://doi.org/10.1016/j.scitotenv.2019.06.090

Tabayashi Y, Koba K (2011) Heterogeneous atmospheric nitrogen deposition effects upon the nitrate concentration of stream waters in a forested mountain area. Water Air Soil Pollut 216:105–115. https://doi.org/10.1007/s11270-010-0519-5

Tabayashi Y, Miki K, Godo T, Yamamuro M, Kamiya H (2017) Multitracer identification of nutrient origin in the Hii River watershed, Japan. Landsc Ecol Eng 13:119–129. https://doi.org/10.1007/s11355-016-0307-5

Tobari Y, Koba K, Fukushima K, Tokuchi N, Ohte N, Tateno R, Toyoda S, Yoshioka T, Yoshida N (2010) Contribution of atmospheric nitrate to stream-water nitrate in Japanese coniferous forests revealed by the oxygen isotope ratio of nitrate. Rapid Commun Mass Spectrom 24:1281–1286. https://doi.org/10.1002/rcm.4498

Toda H, Mochizuki Y, Kawanishi T, Kawashima H (1997) Estimation of reduction in nitrogen load by tea and paddy field land system in Makinohara area of Shizuoka (in Japanese with English abstract). Jpn J Soil Sci Plant Nutr 68:369–375. https://doi.org/10.20710/dojo.68.4_369

Toda H, Uemura Y, Okino T, Kawanishi T, Kawashima H (2002) Use of nitrogen stable isotope ratio of periphyton for monitoring nitrogen sources in a river system. Water Sci Technol 46:431–435. https://doi.org/10.2166/wst.2002.0774

Trenberth KE (2011) Changes in precipitation with climate change. Clim Res 47:123–138. https://doi.org/10.3354/cr00953

Tsunogai U, Komatsu DD, Daita S, Kazemi GA, Nakagawa F, Noguchi I, Zhang J (2010) Tracing the fate of atmospheric nitrate deposited onto a forest ecosystem in Eastern Asia using $\Delta^{17}O$. Atmos Chem Phys 10:1809–1820. https://doi.org/10.5194/acp-10-1809-2010

Westra S, Fowler HJ, Evans JP, Alexander LV, Berg P, Johnson F, Kendon EJ, Lenderink G, Roberts NM (2014) Future changes to the intensity and frequency of short-duration extreme rainfall. Rev Geophys 52:522–555. https://doi.org/10.1002/2014RG000464

Yamada T, Shimizu T, Inoue T, Tachibana H (1999) Storm run-off characteristics of loads of chemical components from forest basins (in Japanese with English abstract). Environ Eng Res 36:217–224. https://doi.org/10.11532/proes1992.36.217

Yoshimoto S, Tsuchihara T, Ishida S, Masumoto T, Imaizumi M (2011) Groundwater flow and transport and potential sources of groundwater nitrates in the Ryukyu limestone as a mixed flow aquifer in Okinawa Island, Japan. Paddy Water Environ 9:367–384. https://doi.org/10.1007/s10333-011-0252-8